



Published in final edited form as:

Biotechnol J. 2015 July ; 10(7): 1067–1081. doi:10.1002/biot.201400665.

Optimization of bioprocess conditions improves production of a CHO cell-derived, bioengineered heparin

Jong Youn Baik^{1,*}, Hussain Dahodwala¹, Eziafa Oduah¹, Lee Talman¹, Trent R. Gemmill^{1,6}, Leyla Gasimli², Payel Datta², Bo Yang³, Guoyun Li³, Fuming Zhang⁴, Lingyun Li³, Robert J. Linhardt^{2,3,4}, Andrew M. Campbell⁵, Stephen F. Gorfien⁵, and T. Sharfstein Susan¹

¹Colleges of Nanoscale Science and Engineering, SUNY Polytechnic Institute, Albany, NY, USA

²Department of Biology and Center for Biotechnology and Interdisciplinary Studies, Rensselaer Polytechnic Institute, Troy, NY, USA

³Department of Chemistry and Chemical Biology and Center for Biotechnology and Interdisciplinary Studies, Rensselaer Polytechnic Institute, Troy, NY, USA

⁴Department of Chemical and Biological Engineering and Center for Biotechnology and Interdisciplinary Studies, Rensselaer Polytechnic Institute, Troy, NY, USA

⁵Thermo Fisher Scientific Inc., Waltham, MA, USA

⁶Albany College of Pharmacy and Health Sciences, Albany, NY, USA

Abstract

Heparin is the most widely used anticoagulant drug in the world today. Heparin is currently produced from animal tissues, primarily porcine intestines. A recent contamination crisis motivated development of a non-animal-derived source of this critical drug. We hypothesized that Chinese hamster ovary (CHO) cells could be metabolically engineered to produce a bioengineered heparin, equivalent to current pharmaceutical heparin. We previously engineered CHO-S[®] cells to overexpress two exogenous enzymes from the heparin/heparan sulfate biosynthetic pathway, increasing the anticoagulant activity ~100-fold and the heparin/heparan sulfate yield ~10-fold. Here, we explored the effects of bioprocess parameters on the yield and anticoagulant activity of the bioengineered GAGs. Fed-batch shaker-flask studies using a proprietary, chemically-defined feed, resulted in ~two-fold increase in integrated viable cell density and 70% increase in specific productivity, resulting in nearly three-fold increase in product titer. Transferring the process to a stirred-tank bioreactor increased the productivity further, yielding a final product concentration of ~90 µg/mL. Unfortunately, the product composition still differs from pharmaceutical heparin, suggesting that additional metabolic engineering will be required. However, these studies clearly demonstrate bioprocess optimization, in parallel with metabolic engineering refinements, will play

Correspondence: Prof. Susan T. Sharfstein, Colleges of Nanoscale Science and Engineering, SUNY Polytechnic Institute, 257 Fuller Road, Albany, NY 12203, USA, ssharfstein@sunycnse.com.

*Current address: Department of Chemical and Biomolecular Engineering and Delaware Biotechnology Institute, University of Delaware, Newark, DE, USA

Conflict of interest

The authors declare no financial or commercial conflict of interest.

a substantial role in developing a bioengineered heparin to replace the current animal-derived drug.

Keywords

CHO cells; Disaccharide analysis; Fed-batch cultures; Glycosaminoglycans; Metabolic engineering

1 Introduction

Heparin (HP) is the most widely used anticoagulant drug in modern medicine; approximately 300,000 doses/day are used in the U.S., and greater than 100 tons of heparin are used annually, with a market value of ~\$7 billion [1, 2]. Heparin is a highly sulfated polysaccharide found covalently attached to the core protein serglycin and stored in intracellular granules of mast cells that are found in the intestines and lungs of many animals [1, 3]. A health crisis in 2008, involving the adulteration of heparin produced from hogs in China, led to the death of ~100 Americans and resulted in a demand for heparin from non-animal sources [4]. In addition, recent studies suggest that heparin may have significant antineoplastic activity, separate and distinct from its anticoagulant activity [5–9], while other studies indicate a role for heparin in treating inflammation, infertility, and infectious disease [10–14]. These observations point to a potential demand for tailored heparin and heparin-like molecules with specific structural and functional properties.

Chinese hamster ovary (CHO) cells are the workhorse of the biopharmaceutical industry. Currently, the biopharmaceuticals market is ~\$130 billion annually with over half of those drugs produced in CHO cells, due to the relative ease of culture and human-like glycosylation patterns. Of the eight best-selling biopharmaceuticals in 2013, five of these drugs are produced in CHO cells (Genetic Engineering News, <http://www.genengnews.com/insight-and-intelligence/the-top-25-best-selling-drugs-of-2013/77900053> March 3, 2014). CHO cells (and all mammalian cells) naturally produce heparan sulfate (HS), a related glycosaminoglycan (GAG) that contains less sulfation and little anticoagulant activity. We hypothesized that CHO cells could be engineered to produce a bioengineered heparin by expressing heparin biosynthetic enzymes that are not naturally expressed in CHO cells [15, 16]. By exogenously expressing two critical biosynthetic enzymes, N-deacetylase/N-sulfotransferase 2 (NDST2) and heparan sulfate 3-O-sulfotransferase 1 (3OST-1), we increased the anticoagulant activity of the engineered HP/HS nearly 100-fold and the amount of HS produced and secreted approximately 10-fold. However, the anticoagulant activity was still much lower than pharmaceutical heparin; the structure was quite different than the pharmaceutical compound, and the productivity (~20 µg/mL) was much lower than typical biopharmaceuticals produced in CHO cells (e.g., antibodies at 1–10 mg/mL). The low productivity is particularly a problem for heparin whose annual demand is ~ 2 orders of magnitude greater than even high volume monoclonal antibodies. However, it is well known that bioprocess optimization for protein therapeutics produced in CHO cells can increase product titers 10- to 100-fold by increasing both specific productivity and integrated viable cell density (IVCD). Hence, we hypothesized that bioprocess optimization for our HP/HS

producing CHO cell lines could substantially improve product titers, a critical step in evaluating the commercial potential of this technology. In addition, process conditions can dramatically affect the glycosylation patterns of recombinant proteins. Increasing dissolved oxygen (DO) has been reported to both increase [17–19] and decrease [20] protein glycosylation across a broad range of cell lines and proteins. An additional study found DO oscillation increased sialylation, branching, and galactosylation [21]. Feeding strategies can also significantly affect glycosylation; in particular, any glucose limitation can significantly affect site occupancy [22–24] and reduce both galactosylation and sialylation [25, 26]. Hence, altering the bioprocess parameters may also impact the GAG structures of proteoglycans, possibly generating more “heparin-like” structures.

In this study, we report the effects of process optimization in fed-batch shake flasks and fed-batch bioreactors on the growth, productivity, and product structures/activity for both parental (CHO-S®) cells and two metabolically engineered clones producing engineered HP/HS GAGs. By optimizing feed compositions, we significantly increased both the specific productivity of the GAGs as well as the IVCD, increasing titers several fold. We observed significant metabolic differences between the engineered cells and the host cells in terms of nutrient uptake and metabolite production. Finally, by altering the feeding strategy to increase the sulfur availability, we were able to increase the anticoagulant activity of the bioengineered heparin, highlighting the importance of bioprocess development in achieving product quality attributes.

2 Materials and Methods

2.1 Batch cell culture

Construction of Dual-3 and Dual-29 cell lines that express NDST2 and 3OST-1 has been previously reported [15]. CHO-S® (Thermo Fisher Scientific Inc. Waltham, MA), Dual-3, and Dual-29 cells were maintained in 125 mL polycarbonate Erlenmeyer flasks (Corning, Corning, NY) containing 25 mL of CD CHO medium (Thermo Fisher Scientific) supplemented with 8 mM GlutaMAX™ (Thermo Fisher Scientific) and 15 mL of hypoxanthine/thymidine solution per 500 mL of medium (HT, Corning Life Sciences, Corning, NY). All cells were seeded at 2×10^5 cells/mL and cultured on orbital shakers agitated at 125 rpm in a humidified 37 °C incubator with 5% CO₂. In addition, 1 mg/mL of Geneticin (G418, Thermo Fisher Scientific) and 500 mg/mL of Zeocin™ (Thermo Fisher Scientific) were added to the medium for dual expressing cell lines. Viable cell densities were determined by trypan blue exclusion using a Bio-Rad TC20™ automated cell counter.

2.2 Fed-batch shaker experiments

Two series of fed-batch shaker flask cultures were performed. In the first series, CHO-S®, Dual-3, and Dual-29 cells were seeded at 2×10^5 cells/mL in 125 mL shaking flasks containing 25 mL of basic culture media described above. Feeding supplements (3 g/L glucose, 3 g/L galactose, or 2.5 mL of CHO CD EfficientFeed™ B (Thermo Fisher Scientific)) were added to each flask on day 3, 5, and 7. A set of control cultures were not fed. Cultures were performed in triplicate. In the second fed-batch series, Dual-29 cells were seeded as above. CHO CD EfficientFeed™ B and glucose were fed to all cultures, with

bolus additions of GlutaMAX™, and/or L-cysteine (L-cysteine-HCl, monohydrate, Sigma) in experimental flasks. The feed volumes and schedule are summarized in supplementary Table S1. Cultures were performed in duplicate. For all experiments, media samples were collected daily, centrifuged, and stored at -20 °C for later analysis.

2.3 Fed-batch bioreactors

Fed-batch cultures were performed in a 2-L Biostat B bioreactor (Sartorius Stedim, Bohemia, NY) with a 1-L working volume. The bioreactor was inoculated at 2×10^5 cells/mL from exponentially growing cultures. The stirring speed was set at 80 rpm and the dissolved oxygen concentration was controlled to be equivalent to 50% of the air saturation. The culture temperature and pH were controlled at 37 °C and at 7.10 ± 0.05 , respectively. 100 mL of CHO CD EfficientFeed™ B was added to the culture on day 3, 5, 7, 9, and 11 for the first run and on day 2, 4, 6, 8, and 10 for the second run. To maintain a sufficient glucose level, 3 g/L of glucose were supplemented when the concentration of glucose was below 3 g/L in the culture medium.

2.4 Metabolic Analysis

Ammonium, potassium, glucose, lactate, glutamate and glutamine concentrations in the culture supernatants were measured using a YSI 7100 (YSI Inc., Yellow Springs, OH) metabolite analyzer according to the manufacturer's manual. For the total glutamine analysis, 1 % (v/v) leucine peptidase (Sigma-Aldrich, St. Louis, MO) was added to the media samples, followed by 2h incubation at 37 °C to cleave GlutaMAX™.

The concentrations of amino acids were determined using the UPLC amino acid method developed by Waters Corporation. Amino acids were derivatized with AccQ•Fluor™ Ultra Reagent (6-aminoquinolyl-N-hydroxysuccinimidyl carbamate) and separated on a bridged ethyl hybrid (BEH) C18 column with 1.7 µm particles using a formate buffer/acetonitrile gradient followed by UV detection at 260 nm. Due to co-elution of multiple component forms, L-cystine cannot be quantitated with this method. However, the qualitative presence of this component can be detected to determine relative levels in the spent medium samples.

2.5 GAG isolation, microcarbazole assays

GAGs in the culture medium were isolated and purified as described previously [15]. Twenty-five microliters of purified GAG samples were mixed with 150 µl of 0.1 % sodium tetraborate dissolved in 98 % sulfuric acid and loaded into a 96-well PCR plate (Thermo Fisher Scientific), followed by incubation at 99 °C for 15 min in a thermocycler. After cooling to 4 °C, 5 µL of 1.25 mg/mL re-crystallized carbazole was added to the GAG samples; the samples were mixed by vortexing and incubated at 99 °C for 15 min. The samples were transferred into a 96-well assay plate (Corning) and the absorbance at 515 nm was measured on a Tecan Infinite M200 plate reader.

2.6 Factor Xa Assays

Factor Xa, antithrombin III (ATIII), and chromogenic substrate (Arg-Gly-Arg-pNA 2HCl) were from a Hemosil fXa assay kit (Instrumentation Laboratory, 0020009400). Additional chromogenic substrate was obtained from Biophen (CS 11(65)). Samples of GAGs were

incubated for 1 hour at room temperature in a 100 μ L volume containing 50 mM Tris, pH 8.4, 0.9% NaCl, 0.001–0.005 IU (typically 0.002) ATIII and 0.01 – 0.05 (typically 0.02) nKat fXa. After incubating, 20 μ L of 0.75 mg/mL chromogenic substrate was added and the absorbance at 410 nM was monitored for one hour in a Tecan Infinite M200 plate reader. All manipulations, with the exception of the addition of the chromogenic substrate were performed using an Eppendorf epMotion 5075 liquid handler. The rate of para-nitroaniline (pNA) release was determined by plotting the nMols of pNA released vs. time and linearizing by assuming the released Arg-Gly-Arg and chromogenic substrate have a similar affinity for fXa. The natural log of the reciprocal of this rate, after subtracting the blank was plotted against the concentration of heparin standards (Sigma-Aldrich, H4787) to generate the standard curve.

2.7 Disaccharide Analysis

GAGs were depolymerized and derivatized with 2-aminoacridine, followed by liquid chromatography mass spectrometry (LC-MS) analysis as previously described [27, 28]. Disaccharide abbreviations are as follows: Δ UA-GlcNAc (0S), Δ UA-GlcNS (NS), Δ UA-GlcNAc6S (6S), Δ UA2S-GlcNAc (2S), Δ UA2S-GlcNS (NS2S), Δ UAGlcNS6S (NS6S), Δ UA2S-GlcNAc6S (2S6S), and Δ UA2SGlcNS6S (TriS) where Δ UA is 4-deoxy-R-L-threo-hex-4-enopyranosyluronic acid.

2.8 RNA extraction and qRT-PCR reaction

Total RNA was extracted from Dual-29 cells on days 2, 4, 6, 8, and 12 of the first bioreactor run and on days 4, 5, 7, 9, and 11 of the second bioreactor run. RNA purification was performed using the RNeasy Mini Kit (Qiagen) in a QIAcube (Qiagen), according to the manufacturer's instructions. Total RNA was quantified using a NanoDrop 2000 Spectrophotometer (Thermo Fischer Scientific). Ninety ng of total RNA per sample was used for reverse transcription PCR using Taqman One Step RT-PCR kit (Thermo Fisher Scientific). The data were normalized to GAPDH housekeeping gene. Probe-primer sequences are given in supplementary Table S2.

2.9 Statistical Analysis

Statistical analysis was performed using GraphPad Prism version 5.00 for Windows, GraphPad Software, San Diego California USA, www.graphpad.com.

3 Results

3.1 Growth and productivity of wild-type CHO-S[®] and bioengineered dual expressing cell lines in batch shaker flask studies

Cells in batch shake-flask studies were grown in CD-CHO, supplemented with 8 mM GlutaMAX[™] and 1.5 \times HT to assess the growth and GAG productivity of the dual expressing clones and identify nutrient limitations. As seen in Figure 1A, the Dual-29 clone exhibited significantly lower maximum viable cell density than the Dual-3 clone or the CHO-S[®] parental cell line. The lower maximum viable cell density was due, in part, to a rapid decrease in cell viability (Figure 1A, ii) with the Dual-29 clone dropping well below 50% viability by 6 days in culture. Despite the low maximum viable cell density, the

specific growth rate of the Dual-29 cell line over the first four days of culture was significantly greater than that of the Dual-3 clone, although not as high as the CHO-S[®] parental cell line (Table 1a). The overall GAG produced by the Dual-29 cell line was comparable to that of CHO-S[®] (Figure 1A, iii), indicating a much higher specific productivity for the Dual-29 clones (Table 1a). We previously reported the disaccharide composition of the GAGs produced by the wild-type and dual expression CHO cell clones [15]. The predominant GAG produced in the CHO-S[®] cell line was unsulfated (OS), although some N-sulfated (NS) and di- and trisulfated forms were also seen, whereas the dual expressing clones showed primarily NS disaccharides. In this study, we examined the change in distribution throughout the culture and noted that in both the parental cell line and the dual expressing clones, there was a shift throughout the culture with a reduction in the disulfated forms and an increase in the OS form (Figure 1B), leading us to hypothesize that there might be limitations in the sulfur availability as the culture progressed.

We next evaluated the nutrient profiles throughout the culture to determine what was potentially limiting the growth and productivity of cultures. As seen in Figure 1C, glucose was entirely depleted in the Dual-29 cultures by day 5 in culture, while some still remained in both the CHO-S and Dual-3 cultures, although the CHO-S[®] culture was depleted by day 7. All three cultures show a relative reduction of cystine/cysteine levels, consistent with our hypothesis that sulfur limitations might be causing the decrease in sulfation as the culture progressed. Other metabolites that were depleted included asparagine, ethanolamine, serine and thiamine. The cultures exhibited fairly typical lactate and ammonia production profiles (Figure 1D) with the Dual-29 cultures exhibiting a “lactate shift” from production to consumption as glucose became depleted, while ammonia production continued in all cultures until terminated at day 7.

3.2 Fed-batch shaker studies of wild-type CHO-S[®] and bioengineered dual expressing cell lines

We initiated a set of fed-batch shake-flask studies examining a variety of carbon sources and proprietary feeds with both of the engineered clones and the parental CHO-S[®] cell line in an effort to improve the growth and productivity of the engineered cell lines. The feeds selected were 3 g/L of glucose, 3 g/L of galactose, and CHO CD EfficientFeed[™] B (Feed B). All cultures were fed every other day, on days 3, 5, and 7. CHO CD EfficientFeed[™] B was added at 10% of the initial culture volume for each feed. CHO CD EfficientFeed[™] B is a concentrated, proprietary mix of nutrients.

All of the feeds improved the IVCD by extending the culture duration or extending the duration and increasing the maximum viable cell density (Figure 2 and Table 1b). The most notable increases in maximum viable cell density occurred with CHO CD EfficientFeed[™] B cultures of the parental CHO-S[®] cell line (Figure 2A) while slight increases in maximum viable cell density were seen in the Dual-3 and Dual-29 clones (Figures 2B and 2C, respectively). The effects of feeding on productivity were not as consistent as the effects on culture density (Figure 2D). Glucose feeding led to a substantial increase in GAG production in the Dual-29 cultures, but had no significant effect the CHO-S[®] or Dual-3 cultures. Galactose had a minimal effect on the Dual-29 cultures and no effect on the CHO-

S[®] or Dual-3 cultures. CHO CD EfficientFeed[™] B increased production across the board, with the most significant effect observed in the Dual-29 cell lines. As indicated in Table 1b, feeding improved both the IVCD and the specific productivity in the Dual-29 cultures while the CHO-S[®] cell line showed only a very modest increase in productivity when fed with CHO CD EfficientFeed[™] B and no increase in productivity under any of the other culture conditions compared with control. The increase in both IVCD and qP for the Dual-29 cultures suggests that nutrient limitations in the batch cultures influenced both the growth and productivity. The effect of glucose alone is quite noteworthy as the product of interest is a glycosaminoglycan; hence, a moderate amount of sugar must be present at all times to serve as a biosynthetic precursor.

We determined the concentrations of glucose, glutamate, free and total glutamine, and lactate and ammonia for the CHO-S[®] and Dual-29 fed batch cultures to further characterize the metabolic behavior of fed-batch shaker flasks and develop a feeding strategy for bioreactor cultures (Figure 3). In the control (no feed) and galactose-fed cultures, glucose was depleted within 6 days in the CHO-S[®] cultures and within 5 days in the Dual-29 cultures (Figure 3A and 3B, respectively). Cultures performed with CHO CD EfficientFeed[™] B exhibited significant fluctuations in glucose concentration, with glucose becoming depleted after ~ 9 days in both the CHO-S[®] and Dual-29. The glucose-fed cultures did not become fully glucose depleted, maintaining a glucose concentration greater than 2 g/L for the entire culture duration.

In the CHO-S[®] cell cultures, the glutamate levels remained relatively steady for the glucose-fed cultures while the other feeding conditions showed increased glutamate (Figure 3C). In all cases, the glutamate concentration remained at a moderate level, between 0.2 and 0.6 g/L throughout the entire culture. In contrast, several of the Dual-29 cultures exhibited significant drops in glutamate, with levels approaching 0 in the glucose- and CHO CD EfficientFeed[™] B-fed cultures (Figure 3D). Interestingly, the galactose-fed cultures showed a moderate increase in glutamate levels in the CHO-S[®] cultures and a return to the initial concentration in the Dual-29 cultures after a mid-culture decrease.

The dipeptide L-alanyl-L-glutamine (GlutaMAX[™]) was used as a glutamine source to reduce the amount of ammonia formed by glutamine degradation. The glutamine is slowly released throughout the culture via the action of cellular aminopeptidases. The free glutamine levels in both cell lines were relatively low for the first 5 days (< 0.2 g/L) and then increased, reaching peak values of 0.1 to 0.35 g/L, depending on the culture conditions (Figure 3E and F). This increase coincided with a substantial increase in viable cell density, presumably providing a source of aminopeptidases. Medium samples were treated with leucine aminopeptidase and re-assayed to determine the total available glutamine (Figures 3G and H). The total glutamine levels were fairly similar for all culture conditions. For the CHO-S[®] cultures, the total glutamine was depleted at ~8 days in culture, with slightly lower levels seen in mid-exponential cultures fed with CHO CD EfficientFeed[™] B, presumably due to higher total and integrated viable cell densities in those cultures (Figure 3G). Coinciding with the overall increased metabolic activity, glutamine levels were more rapidly depleted in the Dual-29 cultures than in the CHO-S[®] despite the lower IVCD, with only slight differences seen between the different feeds (Figure 3H).

All of the cultures, with the exception of the glucose-fed culture, exhibited a lactate shift from lactate production to lactate consumption as the glucose concentration decreased (Figures 3I and 3J). The control, galactose-fed, and CHO CD EfficientFeed™ B cultures exhibited nearly complete lactate consumption during the culture period, and the glucose-fed culture, unsurprisingly, exhibited continuous lactate production throughout the culture duration. Interestingly, the maximum level of lactate produced in the Dual-29 cultures was significantly lower than in the CHO-S® cultures ($P=0.006$, paired t-test, see also Supplementary Figure S2), despite the significantly higher glucose uptake, suggesting that a portion of the glucose was channeled into GAG production.

The ammonia levels were fairly similar for all CHO-S® cultures, with slightly less ammonia produced in the cultures fed with CHO CD EfficientFeed™ B (Figure 3K) ($P<0.001$, two-way ANOVA)). In contrast, the ammonia levels increased steadily in all the Dual-29 cultures (Figure 3L), regardless of feed, reinforcing our observation that the metabolic behavior of the engineered cell lines differed substantially from the parental cells. No significant differences were seen under the different feed conditions in the Dual-29 cultures ($P=0.24$, two-way ANOVA).

3.3 Fed-batch bioreactor studies

Culture in bioreactors often improves growth and productivity, as the cells have improved oxygen mass transfer and superior pH control compared with shake flask studies. However, product quality may be altered as a result of shear, oxygen tension or other process changes. In an effort to increase productivity and to examine the effects of bioreactor culture on the GAG composition, Dual-29 cells were cultured in a two-liter bioreactor with a one-liter initial working volume. Based on the results from fed-batch shaker studies, cells were fed daily, alternating between 10% CHO CD EfficientFeed™ B and 3 g/L of glucose (as needed). Two bioreactor runs were performed as shown in Figure 4. In the first run, agitation speed was maintained flexibly at 80–90 rpm to maintain a dissolved oxygen concentration of 50 % of air saturation, while in the second culture, the agitation speed was initially set at 90 rpm to give a higher gas exchange rate. However, higher shear stress from the increased agitation rate hindered the cell growth at the low cell density, and therefore, we decreased the speed to 80 rpm on day 2 and maintaining that speed for the duration of the culture. The maximum viable cell density was $\sim 4 \times 10^6$ cells/mL, similar to that obtained in fed-batch shaker studies; however, the culture duration was extended to nearly 14 days, yielding an IVCD of 33×10^6 cells/mL*day for the first bioreactor run and 25×10^6 cells/mL*day for the second bioreactor run (Figure 4A, i and ii). The final GAG concentration was approximately 70 µg/mL in run 1 and 90 µg/mL in run 2 (Figure 4A, iii), yielding specific productivities of 2.2 and 3.3 pcd for runs 1 and 2, respectively. The alternating glucose/CHO CD EfficientFeed™ B feeding regimen was able to maintain the glucose concentration > 2 g/L for the entire culture duration, with the exception of some process deviations early in run 1 (Figure 4C, top panel). In both runs, a lactate shift was observed at ~4–6 days in culture, with final lactate concentrations below 1 g/L (Figure 4C, 2nd panel). The total glutamine was depleted somewhat more rapidly than in shake-flask cultures, being completely exhausted by day 5 (Figure 4C, 3rd panel). This coincided with a cessation of cell growth, but did not result in a dramatic decrease in cell viability. Ammonia levels were

significantly lower than in shake-flask studies (Figure 4C, 4th panel) remaining below 0.3 g/L, possibly due to improved oxygen and pH control. The reduced ammonia levels may have contributed to improved culture viability late in culture, allowing for extended culture. Despite the feeding, some components were significantly reduced, particularly cystine/cysteine and ethanolamine (Figure 4D).

3.3.1 GAG composition analysis—As culture conditions are known to affect product quality attributes, we evaluated the disaccharide composition of the GAGs produced in fed-batch bioreactors using LC-MS measurements as previously performed on shake-flask samples. As shown in Figure 4B, fed-batch bioreactor samples showed primarily NS structures, with small amounts of OS and disulfated structures (NS6S and NS2S). No significant amount of trisulfated structures was seen. The disaccharide composition was similar to that observed in fed-batch shaker studies although a smaller fraction of unsulfated GAGs was observed in bioreactors than in shake-flasks. The alteration in disaccharide composition suggests that improved oxygen and pH control does have an effect on disaccharide composition, but not significant enough to dramatically alter sulfation patterns. The “gold-standard” for structural analysis of GAGs is nuclear magnetic resonance (NMR) spectroscopy which also permits identification of chondroitin sulfate/dermatan sulfate GAGs as well as the HP/HS GAGs. With the large volumes of cell culture supernatant available from bioreactor cultures, we were able to confirm the results from disaccharide analysis. In addition, we were able to fractionate the GAGs using anion exchange chromatography, eluting with increasing concentrations of sodium chloride. ¹H NMR spectra are shown in supplementary Figure S1 and GAG distributions are given in supplementary Table S3.

In addition to disaccharide analysis, we evaluated the effects of bioreactor culture on the anticoagulant activity of the engineered heparin as shown in Figure 4E. Interestingly, although the second bioreactor culture produced a higher concentration of GAGs (Figure 4A, iii), the anticoagulant activity was lower in the GAGs obtained from the second bioreactor run (Figure 4E).

3.3.2 Analysis of gene expression patterns—We evaluated the expression of a number of endogenous genes in the HP/HS biosynthetic pathways as well as the NDST2 transgene by quantitative real time PCR (qRT-PCR) to further characterize the physiology of the engineered cell lines in bioreactor culture (Figure 4F). There were a few notable trends observed in both bioreactor runs. First, expression of exostosin glycosyltransferase 2 (EXT2, one of the enzymes responsible for chain elongation) increased throughout the culture. EXT1 showed similar behavior in run 2, but not in run 1. One of the transgenes, NDST2, showed a small decrease throughout the culture, particularly in run 2. The behaviors of the other endogenous genes were less consistent from run to run. Both NDST1 and 2OST were down regulated during the transition from exponential to stationary phase in run 2, but not in run 1. No clear changes were seen in C5 epimerase (C5epi, responsible for converting from glucuronic acid to iduronic acid) or 6OST-1 expression.

3.4 Supplemental feeding to improve sulfation

Based on our observation that sulfation levels decreased with increasing time in culture and our further observation that cystine was substantially reduced in both batch shake-flask and fed-batch bioreactor cultures, we performed a series of Dual-29 fed-batch shaker cultures supplemented with either cysteine, GlutaMAX™, or cysteine and GlutaMAX™ to determine if there was any effect on growth, GAG productivity, activity or structures. All cultures were fed on alternating days with 10% CHO CD EfficientFeed™ B and 3 g/L of glucose, beginning at day 3 in culture. At day 4 in culture, cells were supplemented with a bolus of either 8 mM GlutaMAX™, 1.1 mM cysteine (hydrochloride monohydrate), or both (supplementary Table S1). No bolus was added to control cultures. Cells were harvested after 9 days in culture. The viable cell densities were very similar for all culture conditions (Figure 5A, i). The control culture showed a slightly greater maximum viable cell density and slower drop in viability (Figure 5A, ii) than any of the experimental conditions; however, the IVCD values were not statistically different (Figure 5B, $P=0.10$, one-way ANOVA). The GAG concentrations in each culture were similar, although the cysteine supplemented cultures showed a slightly lower GAG productivity; again this was not statistically significant (Figure 5B, $P=0.47$, one-way ANOVA). Metabolite profiles were also similar between the different cultures (supplementary Figure S3) with the exception of the increase in glutamine in the GlutaMAX™ supplemented cultures. Interestingly, despite the increase in glutamine, the ammonia profiles were largely unchanged between the cultures. As glucose was provided in addition to CHO CD EfficientFeed™ B, glucose levels rose continuously from the onset of feeding until the end of the culture, and lactate levels were maintained at a significantly higher level than in the previous shake flask study in which only CHO CD EfficientFeed™ B was provided (Figure 3J). The higher levels of glucose and lactate may have reduced the IVCD and productivity in these studies when compared with the earlier shake-flask cultures.

Most notably, the anticoagulant activity was significantly increased in the cultures fed with cysteine alone when compared with control ($p = 0.014$, student's t-test) and apparently increased in the combined GlutaMAX™/cysteine feed though this was not statistically significant (Figure 5B, iii). The disaccharide analysis from these experiments showed similar patterns to what was observed in bioreactors (Figure 4B) and in previous shaker-flask studies [15], although shaker flask cultures in general showed higher levels of unsulfated GAGs than bioreactors cultures. Somewhat surprisingly, there was little to no difference in the sulfation levels between the control cultures and those fed with cysteine. If anything, a slight increase in the unsulfated GAGs can be seen (Figure 5C). However, the critical determinant of anticoagulant activity is the presence of the ATIII-binding pentasaccharide moiety containing a 3-*O*-sulfate group on the central glucosamine residue [29, 30]. The presence of this 3-*O*-sulfo group renders the structure resistant to lysis into disaccharides [31]. Hence, an increase in 3-*O*-sulfation may have occurred that cannot be observed by disaccharide analysis.

4 Discussion

4.1 Historical approaches to bioprocess optimization and importance of glycan production

Bioprocess optimization plays a critical role in increasing productivity in bioprocesses. The transition from batch to fed-batch processes has resulted in greater than 20-fold increases in IVCD and nearly 100-fold increases in yield [32]. The change from batch to fed-batch processes has been accompanied by dramatic changes in media formulation, first, eliminating serum in favor of hydrolysates, and more recently, shifting towards chemically-defined media [33, 34]. Chemically-defined media provide the advantages of reproducibility, reduced risk from adventitious agents, and simplified product purification, but may require optimization to achieve high levels of growth and productivity. To address these concerns, specialized feeds have been developed to work in conjunction with the chemically-defined basal media to improve productivity. The focus in developing these media and feeds has been on increasing recombinant protein productivity, while maintaining appropriate product quality attributes. This study, the first to examine the effects of bioprocess conditions on productivity and product quality for a bioengineered glycosaminoglycan, has demonstrated that both productivity and product quality can be improved through process modifications. The importance of synthesizing controlled glycan structures for research and therapeutic applications has been highlighted in several recent reports [35], including a report from the National Academies of Science on the future of glycoscience [36]. If we wish to synthesize large quantities of carbohydrate therapeutics or tailor the glycan structures on a protein therapeutic, understanding the effects of process conditions on glycan structures and productivity is critical. Thus, this report represents a significant first step towards merging bioprocessing with glycoengineering.

4.2 Fed-batch shaker studies of wild-type and engineered CHO cell lines

Our initial batch studies showed that the Dual-29 clone exhibited a much higher nutrient uptake rate for glucose and select amino acids (Figure 1C). As glucose depletion was correlated with a substantial drop in viability, we hypothesized that a fed-batch strategy would extend the culture duration and improve product titers. In parallel studies, we also observed changes in sulfation patterns for GAGs produced in all three cell lines investigated, with a decrease in sulfation with increasing culture duration, suggesting limits in sulfur availability. Our initial optimization focused on comparing different carbon feed sources (glucose and galactose) and a proprietary feed, CHO CD EfficientFeed™ B. While all of the feeds extended the culture duration, the effects of the feeds varied significantly between the feeds and the cell lines (Figure 2 and Table 1b). In general, supplementing with a carbon source alone extended the culture duration, but had little effect on the maximum viable cell density. The CHO-S® cells showed the largest increases in maximum cell density, particularly with the complex feed. Perhaps most striking is the difference in the maximum viable cell densities between the different cell lines. Even with feed supplementation, the maximum viable cell density in the Dual-29 cultures was $\sim 4 \times 10^6$ cells/mL, slightly more than half of that in the Dual-3 cultures and significantly less than half of the maximum viable cell densities in the CHO-S® cultures. Glutamine is an essential nutrient for most cultured mammalian cells unless the cells exogenously express glutamine synthetase. As the initial drop in viable cell density in fed-batch shake-flask cultures coincided with glutamine

depletion, we also explored GlutaMAX™ supplementation (Figure 5A); however, no increase in maximum viable cell density or IVCD was observed. Interestingly, in both the CHO-S® and Dual-29 cultures, a sharp increase in free glutamine was observed at ~6-8 days in culture, presumably due to cell death, releasing aminopeptidases.

While increasing viable cell density and, specifically, IVCD is quite important for improved titers, specific productivity is also crucially important. Of the various feeds we explored, glucose and galactose had the smallest effects on titer (Figure 2D and Table 1b), with no significant difference in any of the galactose cultures and a modest improvement in titer and specific productivity in the glucose-fed Dual-29 culture. Interestingly, glucose feeding alone decreased the specific productivity of GAGs (as well as the titer) in the CHO-S® cell line, possibly due to elevated lactate concentrations (> 2 g/L, Figure 3I). CHO CD EfficientFeed™ B significantly improved both growth and productivity, more than doubling the IVCD in both the CHO-S® and Dual-29 cultures. A modest increase in specific productivity was seen in the CHO-S® cultures fed with CHO CD EfficientFeed™ B, leading to ~ 2-fold increase in GAGs produced by the CHO-S® cells. In contrast, feeding CHO CD EfficientFeed™ B to the Dual-29 cultures, nearly doubled the specific productivity (Table 1b), leading to a greater than 3-fold increase in total GAGs produced from the Dual-29 cultures.

4.3 Metabolic differences between wild-type CHO cells and engineered CHO cell lines

It is well known (at least anecdotally) that different clones producing the same recombinant protein from the same host exhibit different metabolic behaviors [37], and that engineered cell lines exhibit different metabolic behaviors than the parental cell lines. For metabolically engineered cells lines, even greater variation in metabolic behavior might be expected. Dual-29 cultures exhibited higher glucose consumption rates than CHO-S® under all conditions evaluated (Figure 1C, Figures 3A and B). Similar behavior was seen for both glutamate and glutamine (Figure 3). In contrast, the lactate concentrations were lower in both batch and fed-batch cultures (Figure 1D and Figures 3I and J), presumably due to a greater carbon demand to supply the elevated GAG production. Ammonia concentrations, on the other hand, were similar in batch cultures of CHO-S®, Dual-3, and Dual-29, but in fed-batch cultures, Dual-29 cells exhibited higher levels of ammonia than CHO-S®, reaching nearly 0.6 g/L (Figure 3L). However, growth in bioreactors reduced the ammonia concentration to ~0.3 g/L (Figure 4C), suggesting that improved pH control and aeration may improve the metabolic profiles of the cell cultures. Interestingly, providing a bolus addition of GlutaMAX™ or GlutaMAX™ and cysteine did not appear to have any effects on ammonia production (supplementary Figure S3).

4.4 Effects of bioprocessing on product quality attributes

The most critical aspects of producing a bioengineered heparin (beyond yield) are the product quality attributes, namely composition and anticoagulant activity. While all HP/HS GAGs consist of repeating units of glucuronic (or iduronic) acid and N-acetyl-glucosamine (Figure S4), the critical sulfation pattern determines the biological activity. As heparin synthesis is a non-templated process, the sequence depends on the presence, localization, and activity of the various biosynthetic enzymes, the availability of precursors, and the

activity of degradative enzymes (e.g., heparinases and sulfatases). In bioreactor cultures, we observed a greater yield of GAGs in run 2 than in run 1, despite having a significantly greater IVCD in run 1. Hence, the specific productivity in run 2 was significantly higher than in run 1 (3.3 pcd vs. 2.2 pcd, F-test $p < 0.05$). However, the anticoagulant activity of the GAGs obtained from run 2 was approximately half that of run 1 (Figure 4E), suggesting a number of changes in GAG biosynthesis between the two runs. No substantial differences were seen in the disaccharide composition between the two runs (Figure 4B), but as discussed earlier, disaccharide analysis cannot identify the presence of 3-*O*-sulfation in the critical pentasaccharide motif required for anticoagulant activity. As process conditions often affect enzyme expression, particularly of exogenous genes, we evaluated the expression of the various HP/HS biosynthetic enzymes during the bioreactor cultures. In general, there was more variation in gene expression during run 2 than in run 1. Notably, in run 2, the activity of EXT 1, increased throughout the culture. EXT1 and EXT2 are responsible for elongation of the growing GAG chains; however, EXT1 apparently has the biosynthetic capabilities while EXT2 serves as a chaperone [38]. Hence, an increase in EXT1 activity could be responsible for the increase in GAG biosynthesis later in culture in reactor run 2. The variation in the anticoagulant activity is more difficult to explain as both cultures showed a decrease in 3OST-1 activity during the later stages of culture (data not shown). 3OST-1 is the enzyme believed to be responsible for adding the critical 3-*O*-sulfation to create the ATIII-binding pentasaccharide motif in heparin. Hence, a decrease in 3OST-1 activity would likely lead to a decrease in anticoagulant activity. However, since the decreases were similar in both bioreactor runs, proposing a mechanism is difficult. Moreover, it is not clear that 3OST-1 is the only 3-*O* sulfotransferase that can create an anticoagulant molecule, as 3OST-1 $-/-$ knockout mice did not exhibit any coagulation defects [39], and other studies indicate a role for 3OST-5 in generating anticoagulant sites [40]. Other contributing factors would include the availability of sulfur precursors; however, similar reductions in cystine occurred in both cultures (Figure 4D), suggesting that sulfur availability was not the distinguishing factor. Possibly with the larger amount of GAGs produced in run 2, there was less available sulfur, leading to a reduction in sulfation.

In an effort to improve the sulfation level, we performed a final series of fed-batch shaker flask studies incorporating a bolus of either GlutaMAX™, cysteine, or both. Cysteine, in particular, may serve as a source of inorganic sulfate, which is required for production of the activated sulfate donor 3'-phosphoadenosine 5'-phosphosulfate (PAPS) [38]. Cultures that were supplemented with cysteine showed greater anticoagulant activity, but no differences in disaccharide analysis, although the critical 3-*O*-sulfation to create the ATIII-binding pentasaccharide motif in heparin cannot be detected by disaccharide analysis. Interestingly, both the fraction of N-sulfated GAGs and the anticoagulant activity were higher in the bioreactor cultures (with a commensurate decrease in non-sulfated GAGs) when compared with shaker-flask cultures, even those supplemented with cysteine (compare Figures 4 and 5), suggesting that the improved mixing, aeration, and pH control of a bioreactor culture have a beneficial effect on product quality. Unfortunately, we were not able to generate any trisulfated GAGs regardless of culture conditions, suggesting that additional metabolic engineering will likely be required to obtain the desired structures and activity. However, the

present studies indicate that bioprocess manipulations will play a critical role in obtaining adequate yields while maintaining product quality attributes.

Supplementary Material

Refer to Web version on PubMed Central for supplementary material.

Acknowledgements

This work was supported by grants from the National Institutes of Health (R01GM090127) and the National Science Foundation (IIP-1321432). Payel Datta was supported in part by a fellowship from Rensselaer Polytechnic Institute. Jaime Goldfuss and Aaron Schrader at Thermo Fisher Scientific performed the amino acid spent media analysis.

Abbreviations

GAG	glycosaminoglycan
CHO	Chinese hamster ovary
NDST2	N-deacetylase/N-sulfotransferase 2
OST	O-sulfotransferase
HS	heparan sulfate
HP	heparin
IVCD	integrated viable cell density
ATIII	antithrombin III
EXT	exostosin glycosyltransferase
DO	dissolved oxygen

References

1. Bhaskar U, Sterner E, Hickey AM, Onishi A, et al. Engineering of routes to heparin and related polysaccharides. *Appl. Microbiol. Biotechnol.* 2012; 93:1–16. [PubMed: 22048616]
2. Linhardt RJ. Heparin: Structure and Activity. *J. Med. Chem.* 2003; 46:2551–2554. [PubMed: 12801218]
3. Linhardt RJ, Gunay NS. Production and Chemical Processing of Low Molecular Weight Heparins. *Seminars in Thrombosis and Hemostasis.* 1999; 25:5–16. [PubMed: 10549711]
4. Liu H, Zhang Z, Linhardt RJ. Lessons learned from the contamination of heparin. *Natural Product Reports.* 2009; 26:313–321. [PubMed: 19240943]
5. Borsig, L. Heparin as an Inhibitor of Cancer Progression. In: Zhang, L., editor. *Glycosaminoglycans in Development, Health and Disease.* 2010. p. 335–349.
6. Casu B, Naggi A, Torri G. Heparin-derived heparan sulfate mimics to modulate heparan sulfate-protein interaction in inflammation and cancer. *Matrix Biology.* 2010; 29:442–452. [PubMed: 20416374]
7. Maraveyas A, Johnson MJ, Xiao YP, Noble S. Malignant melanoma as a target malignancy for the study of the anti-metastatic properties of the heparins. *Cancer and Metastasis Reviews.* 2010; 29:777–784. [PubMed: 20936327]
8. Robert F. The potential benefits of low-molecular-weight heparins in cancer patients. *Journal of Hematology & Oncology.* 2010; 3

9. Yu LY, Garg HG, Li B, Linhardt RJ, et al. Antitumor Effect of Butanoylated Heparin with Low Anticoagulant Activity on Lung Cancer Growth in Mice and Rats. *Curr. Cancer Drug Targets*. 2010; 10:229–241. [PubMed: 20201787]
10. Li PL, Sheng JZ, Liu YH, Li J, et al. Heparosan-Derived Heparan Sulfate/Heparin-Like Compounds: One Kind of Potential Therapeutic Agents. *Medicinal Research Reviews*. 2013; 33:665–692. [PubMed: 22495734]
11. Potdar N, Gelbaya TA, Konje JC, Nardo LG. Adjunct low-molecular-weight heparin to improve live birth rate after recurrent implantation failure: a systematic review and meta-analysis. *Hum. Reprod. Update*. 2013; 19:674–684. [PubMed: 23912476]
12. Seshadri S, Sunkara SK, Khalaf Y, El-Toukhy T, et al. Effect of heparin on the outcome of IVF treatment: a systematic review and meta-analysis. *Reproductive Biomedicine Online*. 2012; 25:572–584. [PubMed: 23069743]
13. Shastri MD, Peterson GM, Stewart N, Sohal SS, et al. Non-anticoagulant derivatives of heparin for the management of asthma: distant dream or close reality? *Expert Opinion on Investigational Drugs*. 2014; 23:357–373. [PubMed: 24387080]
14. Yadav VK, Saraswat M, Chhikara N, Singh S, et al. Heparin and Heparin Binding Proteins: Potential Relevance to Reproductive Physiology. *Curr. Protein Peptide Sci*. 2013; 14:61–69. [PubMed: 23441896]
15. Baik JY, Gasimli L, Yang B, Datta P, et al. Metabolic engineering of Chinese hamster ovary cells: towards a bioengineered heparin. *Metab. Eng*. 2012; 14:81–90. [PubMed: 22326251]
16. Baik JY, Wang CL, Yang B, Linhardt RJ, et al. Toward a bioengineered heparin: Challenges and strategies for metabolic engineering of mammalian cells. *Bioengineered*. 2012; 3:227–231. [PubMed: 22714556]
17. Chotigeat W, Watanapokasin Y, Mahler S, Gray PP. Role of environmental conditions on the expression levels, glycoform pattern and levels of sialyltransferase for hFSH produced by recombinant CHO cells. *Cytotechnology*. 1994; 15:217–221. [PubMed: 7765934]
18. Lin AA, Kimura R, Miller WM. Production of tPA in recombinant CHO cells under oxygen-limited conditions. *Biotechnol Bioeng*. 1993; 42:339–350. [PubMed: 18613018]
19. Kunkel JP, Jan DCH, Jamieson JC, Butler M. Dissolved oxygen concentration in serum-free continuous culture affects N-linked glycosylation of a monoclonal antibody. *J. Biotechnol*. 1998; 62:55–71. [PubMed: 9684342]
20. Trummer E, Fauland K, Seidinger S, Schriebl K, et al. Process parameter shifting: Part I. Effect of DOT, pH, and temperature on the performance of Epo-Fc expressing CHO cells cultivated in controlled batch bioreactors. *Biotechnol. Bioeng*. 2006; 94:1033–1044. [PubMed: 16736530]
21. Serrato JA, Palomares LA, Meneses-Acosta A, Ramírez OT. Heterogeneous conditions in dissolved oxygen affect N-glycosylation but not productivity of a monoclonal antibody in hybridoma cultures. *Biotechnol Bioeng*. 2004; 88:176–188. [PubMed: 15449295]
22. Hayter PM, Curling EM, Baines AJ, Jenkins N, et al. Glucose-limited chemostat culture of chinese hamster ovary cells producing recombinant human interferon-gamma. *Biotechnol Bioeng*. 1992; 39:327–335. [PubMed: 18600949]
23. Xie L, Nyberg G, Gu X, Li H, et al. Gamma-interferon production and quality in stoichiometric fed-batch cultures of Chinese hamster ovary (CHO) cells under serum-free conditions. *Biotechnol Bioeng*. 1997; 56:577–582. [PubMed: 18642278]
24. Nyberg GB, Balcarcel RR, Follstad BD, Stephanopoulos G, et al. Metabolic effects on recombinant interferon-gamma glycosylation in continuous culture of Chinese hamster ovary cells. *Biotechnol. Bioeng*. 1999; 62:336–347. [PubMed: 10099545]
25. Takuma S, Hirashima C, Piret JM. Dependence on glucose limitation of the pCO₂ influences on CHO cell growth, metabolism and IgG production. *Biotechnol Bioeng*. 2007; 97:1479–1488. [PubMed: 17318909]
26. Wong DCF, Wong KTK, Goh LT, Heng CK, et al. Impact of dynamic online fed-batch strategies on metabolism, productivity and N-glycosylation quality in CHO cell cultures. *Biotechnol. Bioeng*. 2005; 89:164–177. [PubMed: 15593097]

27. Volpi N, Galeotti F, Yang B, Linhardt RJ. Analysis of glycosaminoglycan-derived, precolumn, 2-aminoacridone-labeled disaccharides with LC-fluorescence and LC-MS detection. *Nature Protocols*. 2014; 9:541–558. [PubMed: 24504479]
28. Yang B, Chang Y, Weyers AM, Sterner E, et al. Disaccharide analysis of glycosaminoglycan mixtures by ultra-high-performance liquid chromatography-mass spectrometry. *J. Chromatogr. A*. 2012; 1225:91–98. [PubMed: 22236563]
29. Atha D, Lormeau J-C, Petitou M, Rosenberg R, et al. Contribution of monosaccharide residues in HP binding to antithrombin III. *Biochemistry*. 1985; 24:6723–6729. [PubMed: 4084555]
30. Lindahl U, Backstrom G, Thunberg L, Leder I. Evidence for a 3-O-sulfated D-glucosamine residue in the antithrombin-binding sequence of HP. *Proc. Natl. Acad. Sci. (USA)*. 1980; 77:6551–6555. [PubMed: 6935668]
31. Li G, Yang B, Li L, Zhang F, et al. Analysis of 3-O-sulfo group-containing heparin tetrasaccharides in heparin by liquid chromatography-mass spectrometry. *Anal. Biochem*. 2014; 455:3–9. [PubMed: 24680753]
32. Wurm FM. Production of recombinant protein therapeutics in cultivated mammalian cells. *Nat Biotechnol*. 2004; 22:1393–1398. [PubMed: 15529164]
33. Zhang HF, Wang HB, Liu M, Zhang T, et al. Rational development of a serum-free medium and fed-batch process for a GS-CHO cell line expressing recombinant antibody. *Cytotechnology*. 2013; 65:363–378. [PubMed: 22907508]
34. Burky JE, Wesson MC, Young A, Farnsworth S, et al. Protein-free fed-batch culture of non-GS NS0 cell lines for production of recombinant antibodies. *Biotechnol. Bioeng*. 2007; 96:281–293. [PubMed: 16933323]
35. Shriver Z, Raguram S, Sasisekharan R. Glycomics: a pathway to a class of new and improved therapeutics. *Nat Rev Drug Discov*. 2004; 3:863–873. [PubMed: 15459677]
36. Academies, N.R.C.o.t.N.. Transforming Glycoscience: A Roadmap for the Future. Washington, DC: 2012.
37. Dahodwala H, Nowey M, Mitina T, Sharfstein S. Effects of clonal variation on growth, metabolism, and productivity in response to trophic factor stimulation: a study of Chinese hamster ovary cells producing a recombinant monoclonal antibody. *Cytotechnology*. 2012; 64:27–41. [PubMed: 21822681]
38. Carlsson, P.; Kjellén, L. Heparin Biosynthesis. In: Lever, R.; Mulloy, B.; Page, CP., editors. *Heparin - A Century of Progress*. Berlin Heidelberg: Springer; 2012. p. 23-41.
39. Shworak, NW.; Kobayashi, T.; Agostini, Ad; Smits, NC. Anticoagulant Heparan Sulfate: To Not Clot—Or Not?. In: Lijuan, Z., editor. *Progress in Molecular Biology and Translational Science*. Academic Press; 2010. p. 153-178.
40. Thacker BE, Xu D, Lawrence R, Esko JD. Heparan sulfate 3-O-sulfation: A rare modification in search of a function. *Matrix Biology*. 2014; 35:60–72. [PubMed: 24361527]

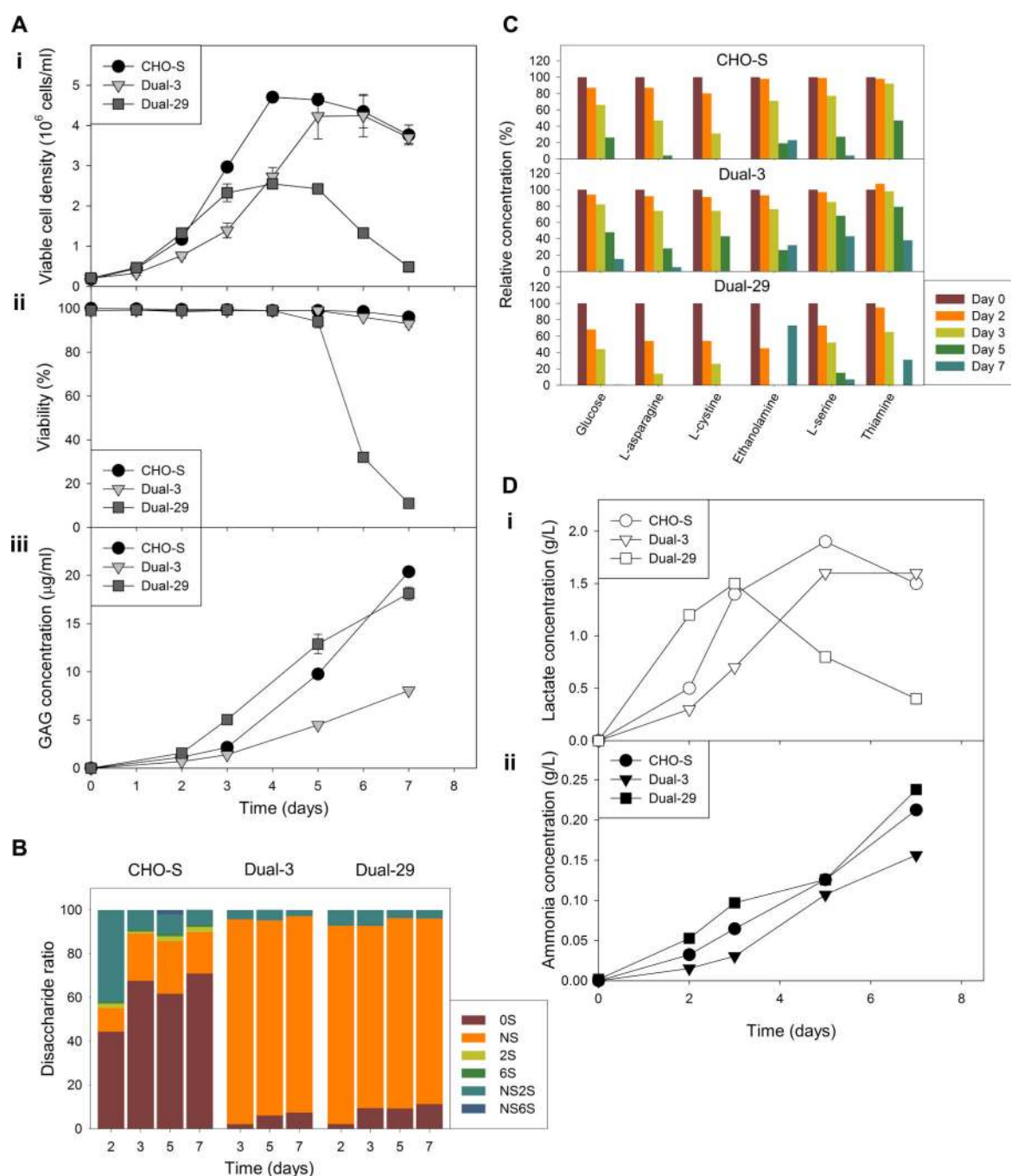
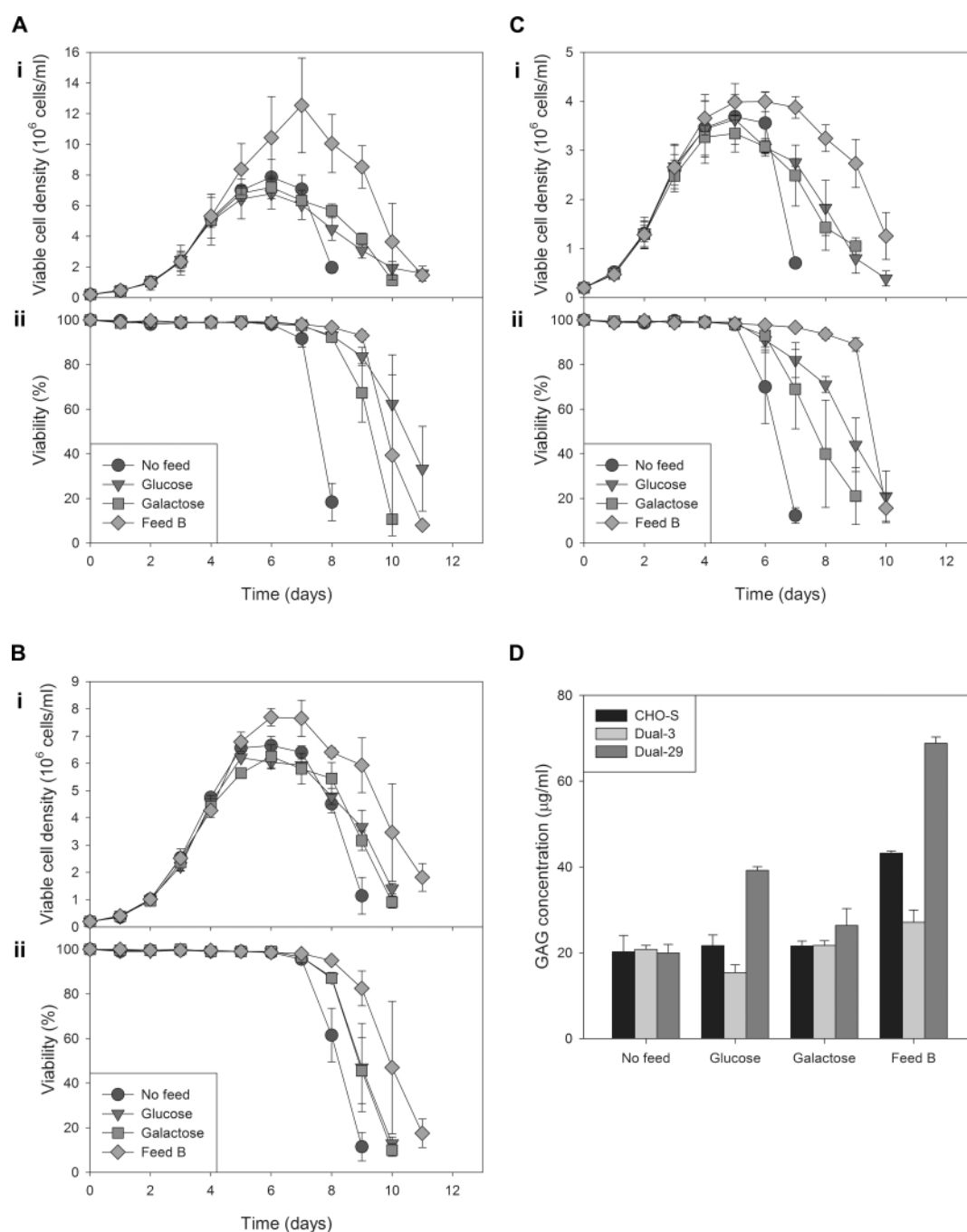


Figure 1.

Growth, productivity and metabolism of CHO-S[®], Dual-3, and Dual-29 cell lines in batch shaker-flask cultures. Viable cell densities were determined by trypan blue exclusion using a Bio-Rad TC20[™] automated cell counter; GAG concentrations were determined by carbazole assay on purified GAGs; disaccharide analysis was performed by LC-MS; metabolite analysis was performed using a YSI 7100 metabolite analyzer or by UPLC amino acid analysis. (A) Viable cell density (i), viability (ii), and medium GAG concentrations (iii). (B) Disaccharide composition of GAGs purified from cell culture medium. (C) Relative

concentrations of selected metabolites. (D) Lactate (i) and ammonia (ii) concentrations. Error bars represent the standard deviation of duplicate biological samples.

**Figure 2.**

Growth and productivity of CHO-S[®], Dual-3, and Dual-29 cell lines for control (no feed) and three different feed supplements (glucose, galactose, or CHO CD EfficientFeed[™] B) in fed-batch shaker-flask cultures. Feeds were added on days 3, 5 and 7. Viable cell densities and GAG concentrations were determined as described in Figure 1. (A) Viable cell densities (i) and viabilities (ii) of CHO-S[®] cultures. (B) Viable cell densities (i) and viabilities (ii) of Dual-3 cultures. (C) Viable cell densities (i) and viabilities (ii) of Dual-29 cultures. (D)

GAG productivities. Error bars represent the standard deviation of triplicate biological samples.

Author Manuscript

Author Manuscript

Author Manuscript

Author Manuscript

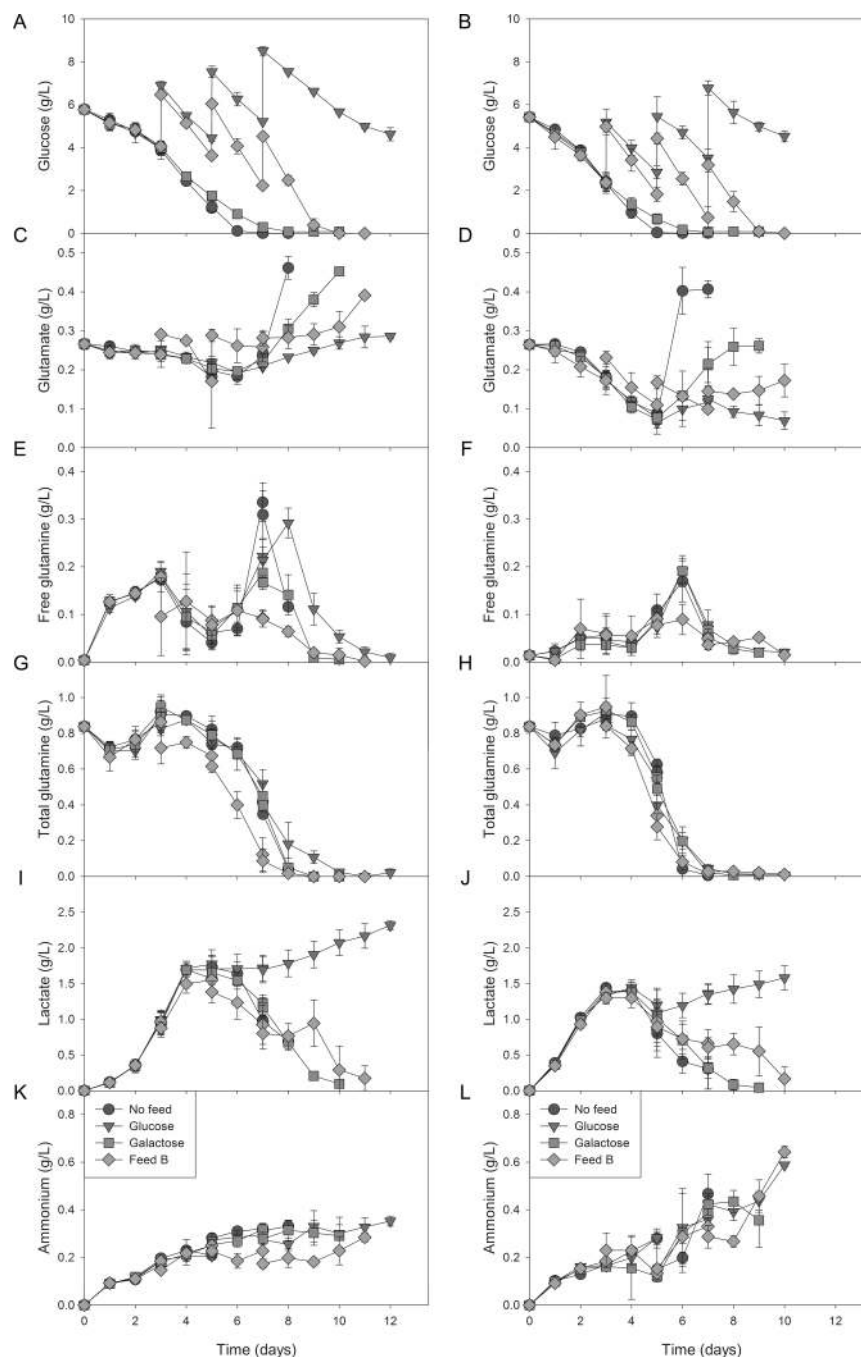
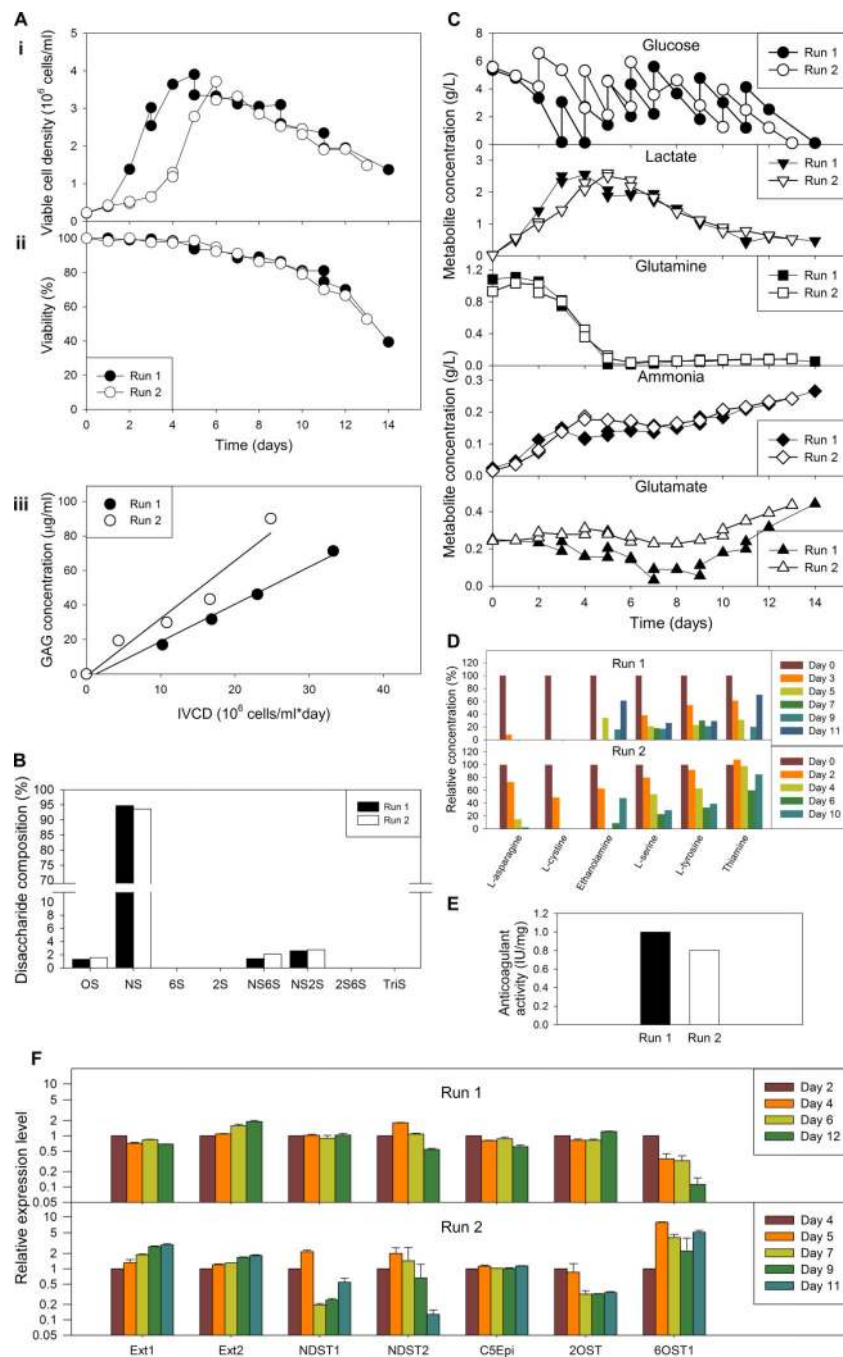


Figure 3. Nutrient and waste metabolite concentrations from CHO-S[®] (left panels) and Dual-29 (right panels) fed-batch shaker-flask cultures described in Figure 2. Metabolite analysis was performed using a YSI 7100 metabolite analyzer. (A) and (B) glucose; (C) and (D) glutamate; (E) and (F) free glutamine; (G) and (H) total glutamine; (I) and (J) lactate; (K) and (L) ammonia. Error bars represent the standard deviation of triplicate biological samples.

**Figure 4.**

Fed-batch bioreactor cultures of Dual-29 cell line performed in a 2-L Biostat B bioreactor with a 1-L working volume using two feeding strategies. Anticoagulant activity of purified GAGs was determined using a Hemosil fXa assay kit. Gene expression levels were determined by qRT-PCR. (A) Viable cell density (i), viability (ii), and GAG productivity (iii). (B) Disaccharide composition of GAGs purified from culture medium. (C) Metabolite profiles for glucose, lactate, total glutamine, ammonia, and glutamate. (D) Metabolite profiles for selected amino acids, ethanolamine, and vitamins. (E) Anticoagulant activity

normalized to 180 IU/mg for pharmaceutical heparin. (F) Relative gene expression for heparin/heparan sulfate biosynthetic enzymes by qRT-PCR. Error bars in (F) represent the standard deviation of technical replicates.

Author Manuscript

Author Manuscript

Author Manuscript

Author Manuscript

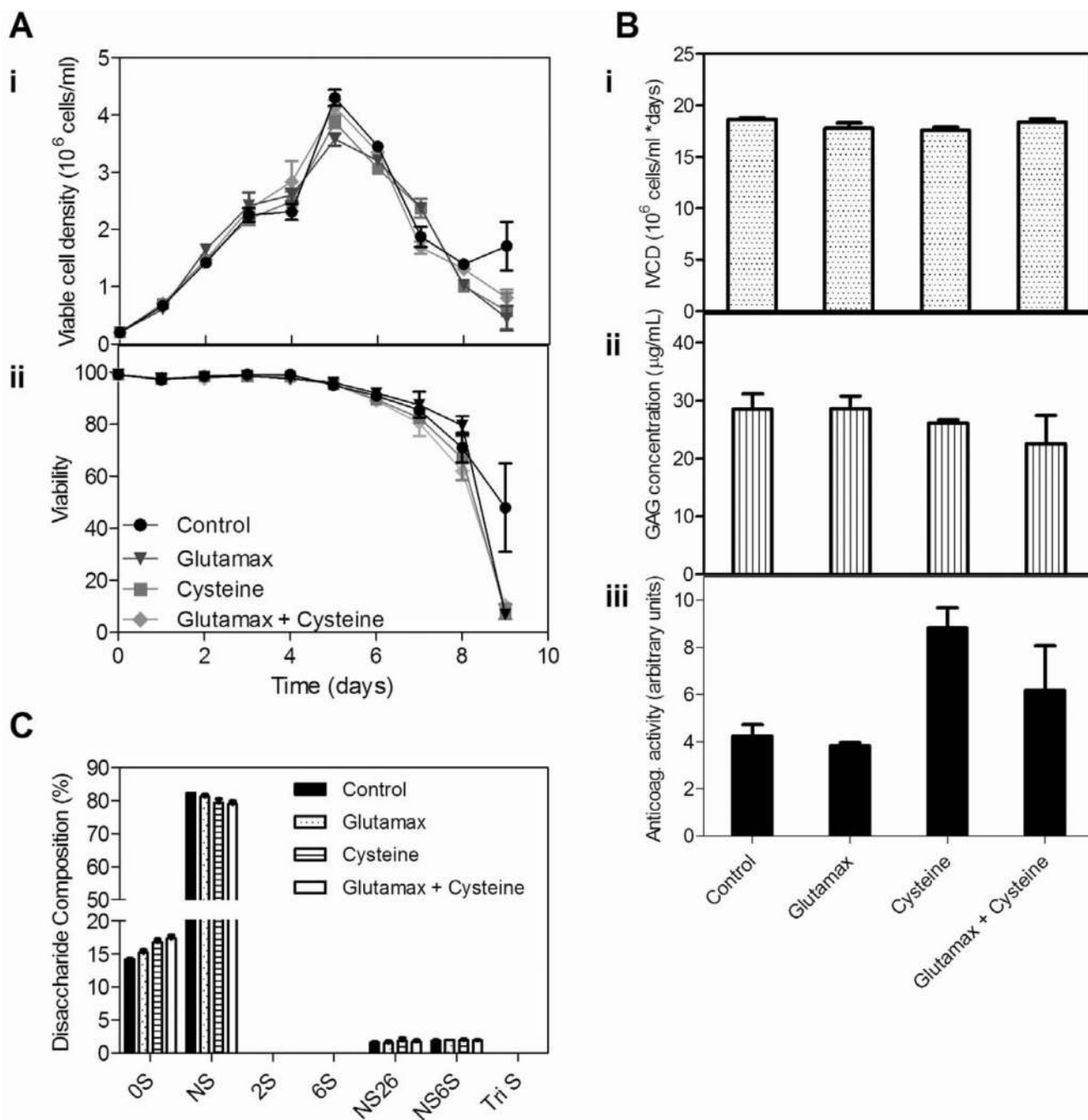


Figure 5. Growth and GAG productivity for Dual-29 cells cultured in fed-batch shaker-flasks with additional GlutaMAX™ or cysteine supplementation as described in Table S1. (A) Viable cell densities (i) and viability (ii); (B) Integrated viable cell densities (i), GAG concentrations for GAGs purified from medium (ii), and relative anticoagulant activity (iii); (C) Disaccharide composition of GAGs purified from cell culture medium. Error bars represent the standard deviation of duplicate biological samples.

Table 1

a. Growth and productivity characteristics in batch shaker-flask cultures shown in Figure 1. Mean \pm SD; n = 2.				
	IVCD (10^6 cells/ml*day)	Specific growth rate (day^{-1})	GAG amount ($\mu\text{g/ml}$)	Specific productivity (pcd)
CHO-S®	20.79 \pm 3.27	0.907 \pm 0.038	20.34 \pm 0.18	1.009 \pm 0.160
Dual-3	17.41 \pm 1.60	0.704 \pm 0.055	8.05 \pm 0.13	0.495 \pm 0.045
Dual-29	10.38 \pm 0.46	0.791 \pm 0.035	18.12 \pm 0.68	1.708 \pm 0.115

b. Effects of various feeds on growth and productivity in fed-batch shaker-flask studies shown in Figure 2. Mean \pm SD; n = 3.				
		IVCD (10^6 cells/ml*day)	GAG amount ($\mu\text{g/ml}$)	Specific productivity (pcd)
CHO-S®	Control	32.2 \pm 1.1	20.2 \pm 3.8	0.626 \pm 0.108
	Glucose	39.4 \pm 6.2	21.6 \pm 2.5	0.564 \pm 0.149
	Galactose	39.4 \pm 3.2	21.6 \pm 1.2	0.552 \pm 0.073
	EfficientFeed™ B	62.3 \pm 9.5	43.2 \pm 0.5	0.704 \pm 0.099
Dual-3	Control	33.0 \pm 1.8	20.8 \pm 1.0	0.628 \pm 0.004
	Glucose	35.3 \pm 0.9	15.3 \pm 1.9	0.434 \pm 0.041
	Galactose	34.8 \pm 2.9	21.7 \pm 1.1	0.624 \pm 0.020
	EfficientFeed™ B	46.5 \pm 1.78	27.1 \pm 2.8	0.582 \pm 0.039
Dual-29	Control	15.5 \pm 1.4	20.0 \pm 2.0	1.298 \pm 0.211
	Glucose	20.0 \pm 1.9	39.2 \pm 0.9	1.964 \pm 0.149
	Galactose	18.0 \pm 0.7	26.3 \pm 4.0	1.457 \pm 0.196
	EfficientFeed™ B	30.1 \pm 0.7	68.8 \pm 1.5	2.287 \pm 0.081